Atmos. Chem. Phys. Discuss., https://doi.org/10.5194/acp-2018-1298
Manuscript under review for journal Atmos. Chem. Phys.
Discussion started: 20 December 2018

Atmospheric Chemistry and Physics Discussions

Investigation of CATS aerosol products and application toward global diurnal variation of aerosols

Logan Lee[1], Jianglong Zhang[1], Jeffrey S. Reid[2], and John E. Yorks[3]

[1]Department of Atmospheric Sciences, University of North Dakota, Grand Forks, ND

[2]Marine Meteorology Division, Naval Research Laboratory, Monterey, CA

[3]NASA Goddard Space Flight Center, Greenbelt, MD

Submitted to

ACP

Dec. 2018

Corresponding Author: jzhang@atmos.und.edu; logan.p.lee@und.edu

Atmos. Chem. Phys. Discuss., https://doi.org/10.5194/acp-2018-1298
Manuscript under review for journal Atmos. Chem. Phys.
Discussion started: 20 December 2018

Atmospheric Chemistry and Physics Discussions

Abstract

We present a comparison of 1064 nm aerosol optical depth (AOD) and aerosol extinction profiles from the Cloud-Aerosol Transport System (CATS) Level 2 aerosol product with collocated Aerosol Robotic Network (AERONET) AOD, Aqua and Terra Moderate Imaging Spectroradiometer (MODIS) Dark Target (AOD) and Cloud-Aerosol Lidar with Orthogonal Polarization (CALIOP) AOD and extinction data for the period of Feb. 2015-Oct. 2017. Upon quality assurance checks of CATS data, reasonable agreements are found between aerosol data from CATS and other sensors. Using quality assured CATS aerosol data, for the first time, variations in AODs and aerosol extinction profiles are evaluated at 00, 06, 12, and 18 UTC (and/or 0:00 am, 6:00 am, 12:00 pm and 6:00 pm local solar times) on both regional and global scales. This study suggests that marginal variations are found in AOD from a global mean perspective, with the maximum and minimum aerosol vertical profiles found at local noon and 6:00 pm local time respectively, for both the June-November and December-May seasons. Strong diurnal variations are found over North Africa and India for the December-May season, and over North Africa, Middle East, and India for the June-November season. In particular, over North Africa, during the June-November season, a diurnal peak in aerosol extinction profile of 20% larger than daily mean is found at 6:00 am (early morning local time), which may possibly be associated with dust generation through the breaking down of low level jet during morning hours.

Atmos. Chem. Phys. Discuss., https://doi.org/10.5194/acp-2018-1298
Manuscript under review for journal Atmos. Chem. Phys.
Discussion started: 20 December 2018

1.0 Introduction

Aerosol measurement through the sun-synchronous orbits of Terra and Aqua by nature encourages a larger scale, daily average point of view. Yet, we know that pollution (e.g., Zhao et al., 2009; Tiwarl et al., 2013; Kaku et al., 2018), fires and smoke properties (e.g., Reid et al., 1999; Giglio et al., 2003; Hyer et al., 2013), and dust (e.g., Mbourou, et al., 1997; Fielder et al., 2013; Heinold et al., 2013) can exhibit strong diurnal behavior. Sun-synchronous passive satellite aerosol observations from the solar spectrum only provide a small sampling of the full diurnal cycle and geostationary sensors such as the Advanced Himawari Imager (AHI) on Himawari 8 (Yoshida et al., 2018) and Advanced baseline Imager on GOES-16/17 (Aerosol Product Application Team of the AWG Aerosols/Air Quality/Atmospheric Chemistry Team, 2012) satellites, while an improvement over their predecessors, must overcome the broader range of scattering and zenith angles (Wang et al., 2003; Christopher and Zhang, 2002) with no nighttime retrievals. AErosol RObotic NETwork (AERONET; Holben et al., 1998) based sun photometer studies improve sampling, but until very recently with the development of a prototype lunar photometry mode, are also limited to daylight hours. The critical early morning and evening are largely missed in solar observation based approaches.

Observation-based diurnal variations of aerosol properties are needed for improving chemical transport modeling, geochemical cycles and ultimately climate. The measurement of diurnal variations of aerosol properties resolved in the vertical is especially crucial of aerosol phenomena for visibility and particulate matter forecasts. Indeed, the periods around sunrise and sunset show significant near surface variability that is difficult to detect with passive sensors. While lidar data from Cloud-Aerosol Lidar with Orthogonal Polarization (CALIOP) provide

early afternoon and morning observations, two temporal points and a 16 day repeat cycle are insufficient to evaluate the morning and evening hours.

Some of the limiting factors in previous studies can be addressed by the Cloud-Aerosol Transport System (CATS) lidar flying aboard the International Space Station (ISS) since 2015 (McGill et al. 2015). The ISS's precessing orbit with a 51.6° inclination allows for 24 hour sampling of the tropics to mid-latitudes, with the ability to observe aerosol and cloud vertical distributions at both day and night time with high temporal resolution. For a given location within ±51.6° (Latitude), after aggregating roughly 60 days of data, near full diurnal cycle of aerosol and cloud properties can be obtained from CATS observations (Yorks et al. 2016). This provides a new opportunity for studying diurnal variations (day and night) in aerosol vertical distributions from space observations.

Use of CATS has its own challenges. Most importantly, CATS retrievals must cope with variable solar noise around the terminator where we expect the strongest diurnal variability to exist. Further, CATS lost its 532 nm channel early in its deployment, leaving only a 1064 nm channel functioning. The availability of only one wavelength limited the CATS cloud-aerosol discrimination algorithm, which can cause a loss of accuracy compared to CALIPSO which has 2 wavelengths. This deficiency is in part overcome by using the Feature Type Score. Using two years of observations from CATS, in this paper, we focus on understanding of the following questions: How well do CATS derived aerosol optical depth (AOD) and aerosol vertical distributions compare with aerosol properties derived from other ground-based and satellite observations such as AERONET, MODIS and CALIOP? Do differences exhibit a diurnal cycle? What are the diurnal variations of aerosol optical depth on a global domain? What are the diurnal variations of aerosol vertical distribution on both regional and global scales?

Atmos. Chem. Phys. Discuss., https://doi.org/10.5194/acp-2018-1298
Manuscript under review for journal Atmos. Chem. Phys.
Discussion started: 20 December 2018

2.0 Datasets

Four datasets, including ground-based AERONET data, as well as satellite retrieved aerosol properties from MODIS and CALIOP, are used for inter-comparing with AOD and aerosol vertical distributions from CATS. Upon thorough evaluation and quality assurance procedures, CATS data are further used for studying diurnal variations of AOD and aerosol vertical distributions for the period of Feb. 2015 – Oct. 2017.

2.1 CATS

CATS Level 2 (L2) Version 2-01 5 km Aerosol Profile products (L20_D-M7.2-V2-01_5kmPro, L20_N-M7.2-V2-01_5kmPro) were used in this study for the entire period of CATS operation on the ISS (~Feb. 2015–Oct. 2017). CATS L2 profile data are provided at 5 km along-track horizontal resolution and 533 vertical levels at 60 m vertical resolution and a wavelength of 1064 nm. CATS also provides data at 532 nm, but due to a laser-stabilization issue, 532 nm data is not recommended for use (Yorks et al. 2016). Thus, only 1064 nm products were used in this study. CATS data are quality-assured following a manner similar to Campbell et al. (2012), which was applied to CALIOP. QA thresholds (including extinction QC flag, Feature Type Score, and uncertainty in extinction coefficient) are listed below:

(a) Extinction_QC_Flag_1064_Fore_FOV is equal to 0

(b) Feature_Type_Fore_FOV = 3 (aerosol only)

(c) -10 <= Feature_Type_Score_FOV <= -2

(d) Extinction_Coefficient_Uncertainty_1064_Fore_FOV <= 10 km^{-1}

Extinction was also constrained to the nominal range provided in the CATS data catalog (0 <= Extincton_Coefficient_1064_Fore_FOV <= 1.25 km -1), similar to several previous studies (Redemann et al., 2012; Toth et al., 2016). Due to the presence of a large amount of near zero negative extinction values, profiles containing these values were also considered by setting all near zero negative values to zero, resulting in an effective threshold of Extinction_Coefficient_1064_Fore_FOV <= 1.25 km^{-1}. For this study, both the Aerosol_Optical_Depth_1064_Fore_FOV and Extinction_Coefficient_1064_Fore_FOV datasets were used to provide AOD and 1064 nm extinction profiles (hereafter the term "extinction" will refer to 1064 nm unless explicitly stated otherwise), respectively.

2.2 CALIOP

NASA's CALIOP is an elastic backscatter lidar that operates at both 532 nm and 1064 nm wavelengths (Winker et al., 2009). Being a part of the A-Train constellation (Stephens et al., 2002), CALIOP provides both day- and night-time observations of Earth's atmospheric system, at a sun-synchronous orbit, with a narrow swath of around 70 m and a temporal resolution of ~16 days (Winker et al., 2009). For this study, CALIOP Level 2.0 5 km Aerosol Profile products (L2_05kmAProf) are used for inter-comparing to CATS retrieved AODs and aerosol vertical distributions.

L2_05kmAProf data are available at 5 km horizontal resolution along-track and include aerosol retrievals at both 532 nm and 1064 nm wavelengths. The vertical resolution is 60 m near-surface, increasing to 180 m above 20.2 km in MSL altitude. As only 1064 nm CATS data are used in this study as mentioned above, likewise only those CALIOP parameters relating to 1064 nm are used in this study (Vaughan et al., 2018; Omar et al., 2013). Note that as suggested

Atmos. Chem. Phys. Discuss., https://doi.org/10.5194/acp-2018-1298
Manuscript under review for journal Atmos. Chem. Phys.
Discussion started: 20 December 2018

by Rajapakshe et al. (2017), lower single to noise ratio (SNR) and higher minimum detectable backscatter are found for the CALIOP 1064 nm data in-comparing with the CALIOP 532 nm data. Also, the CALIOP aerosol layers are detected at 532 nm and the 1064 nm extinction is only computed for the bins within these layers. This may introduce a bias for aerosol above cloud studies. In this study, Extinction_Coefficient_1064 and Column_Optical_Depth_Tropospheric_Aerosols_1064 are used for CALIOP extinction and AOD retrievals, respectively (Vaughan et al., 2018; Omar et al., 2013). As with the CATS data, CALIOP data are quality-assured following the quality assurance steps as mentioned in a few previous studies (e.g. Campbell et al., 2012; Toth et al., 2016; 2018). These QA thresholds are listed below:

(a) Extinction_QC_Flag_1064 is equal to 0,1,2,16, or 18

(b) Atmospheric_Volume_Description = 3 (aerosol only)

(c) -100 <= CAD_Score <= -20

(d) Extinction_Coefficient_Uncertainty_1064 <= 10 km^{-1}

Furthermore, as in Campbell et al. (2012), only those profiles with AOD > 0 were retained in order to avoid profiles composed of only retrieval fill values. Extinction was also constrained to the nominal range provided in the CALIOP data catalog (Extinction_1064 <= 1.25 km -1), similar to our QA procedure for CATS as described above.

2.3 MODIS Collection 6.1 Dark Target product

Moderate Resolution Imaging Spectroradiometer (MODIS) Aqua and Terra Collection 6.1 Dark Target over-ocean AOD data (Levy et al., 2013) were used for comparison to CATS AOD. The data field of "Effective_Optical_Depth_Best_Ocean" were used and only those data

flagged as "good" or "very good" by the Quality_Assurance_Ocean runtime QA flags are selected for this study, similar to Toth et al. (2018). Because MODIS does not provide AOD in the 1064 nm wavelength, AOD retrievals from 860 and 1240 nm spectral channels are used to interpolate AODs at 1064 nm, assuming a constant angstrom exponent as suggested by Shi et al., (2011; 2013). Only totally cloud free (or cloud fraction equal to zero) retrievals, as indicated by the Cloud_Fraction_Land_Ocean parameter are used.

2.4 AERONET

By measuring direct and diffuse solar energy, AERONET observations are used for retrieving AOD and other ancillary aerosol properties such as size distributions (Holben et al., 1998). AERONET data are considered as the ground truth for evaluating CATS retrievals in this study. Only cloud screened and quality assured version 3 level 2 AERONET data at the 1020 nm spectrum are selected and are used for inter-comparing with CATS AOD retrievals at the 1064 nm wavelength. AERONET does not have specific guidance on error in the 1020 nm channel, as it is known to have some thermal sensitivities. However they do report significantly more confidence in version 3 of the data, which has temperature correction (Giles et al., 2018). Error models are ongoing, and for this study we assume double the RMSE, or +/-0.03.

3.0 Results & Discussion

3.1 Inter-comparison of CATS data with AERONET, MODIS and CALIOP data

In this sub-section, the performance of over land and over ocean CATS AOD retrievals are compared against AERONET and C6.1 over ocean MODIS DT aerosol products. CATS

182 derived aerosol extinction vertical distributions are also cross-compared against collocated
183 CALIOP aerosol extinction vertical distributions.
184
185 **3.1.1 CATS-AERONET**
186 As the initial check, CATS data from Feb. 2015-Oct. 2017 are spatially (within 0.4
187 degree Latitude and Longitude) and temporally (±30minutes) collocated against ground-based
188 AERONET data. Note that one AERONET measurement may be associated with several CATS
189 retrievals in both space and time, and vice versa. Thus, both CATS and AERONET data are
190 further averaged spatially and temporally, which results in only one pair of collocated and
191 averaged CATS and AERONET data for a given collocated incident. Also, only data pairs with
192 AOD larger than 0 from both instruments are used for the analysis. This step is necessary to
193 exclude CATS profiles with all retrieval fill values as discussed in Section 2 (Toth et al., 2018).
194 Note that the CATS-AERONET comparisons are for daytime only, and higher uncertainties are
195 expected for CATS daytime than night AODs.
196 As shown in Figure 1a, without quality-assurance procedures, high spikes in CATS AOD
197 of above 1 (1064 nm) can be found for collocated AERONET data with AOD less than 0.3 (1020
198 nm). Those high spikes in CATS AOD may due to cloud contamination in the V2-01 CATS
199 daytime data, which will be improved in the upcoming CATS V3-00 data products. Upon
200 completion of the QA steps as outlined in Section 2.1, a reasonable agreement is found between
201 quality-assured CATS (1064 nm) vs. AERONET (1020 nm) AODs with a correlation of 0.64
202 (Figure 1b). Comparing Figure 1a with 1b, with the loss of only ~10% of collocated pairs due to
203 the QA procedures, we have observed an overall improvement in correlation between CATS and
204 AERONET AOD from 0.17 to 0.64. Note that similar results are found in comparisons between

205 collocated CATS and MODIS/CALIOP data without the use of QA procedures on CATS data.
206 Thus, only QAed CATS data are used hereafter. Still, this exercise highlights the need for
207 careful quality checks of the CATS data before applying the CATS data for advanced
208 applications to overcome cloud-aerosol discrimination uncertainties.
209
210 **3.1.2 CATS-MODIS**
211 To examine over ocean performance, column integrated CATS AODs are inter-compared
212 with collocated Terra and Aqua C6.1 MODIS DT over ocean AOD, interpolated to 1064 nm.
213 Over ocean C6.1 MODIS DT data are selected due to the fact that higher accuracies are reported
214 for over ocean versus over land MODIS DT AOD retrievals (Levy et al., 2013). In addition,
215 comparing with over land MODIS DT data, which provides AOD retrievals at three discrete
216 wavelengths (0.46, 0.55 and 0.65 μm), over water AOD retrievals are available from 7
217 wavelengths including the 0.87 and 1.24 μm spectral channels, allowing a comparison with
218 CATS AOD at the same wavelength upon interpolation.
219 MODIS and CATS AOT retrievals are collocated for the study period of Feb. 2015-Oct.
220 2017 (Figure 2). Pairs of CATS and MODIS data were first selected for both retrievals that fall
221 within ±30 minutes and 0.4 degrees latitude and longitude of each other. Then, similar to the
222 AERONET and CATS collocation procedures, collocated pairs were further averaged to
223 construct one pair of collocated MODIS and CATS data for a given collocation incident. Shown
224 in Figure 2a, a correlation of 0.71 is found between collocated over water Terra MODIS C6.1
225 DT and CATS AODs with a slope of 0.78. Similar results are found for the comparisons
226 between over water Aqua MODIS and CATS AODs with a correlation of 0.75 and a slope of
227 0.79.

Atmos. Chem. Phys. Discuss., https://doi.org/10.5194/acp-2018-1298
Manuscript under review for journal Atmos. Chem. Phys.
Discussion started: 20 December 2018

228

229 **3.1.3 CATS-CALIOP AOD**

230 In the previous two sections, AODs from CATS are inter-compared with retrievals from
231 passive-based sensors such as MODIS and AERONET. In this section, AOD data from
232 CALIOP, which is an active-based sensor, are evaluated against AOD retrievals from CATS.
233 Again, for each collocation incident, pairs of CALIOP and CATS data are selected in which both
234 retrievals fall within ±30 minutes temporally and 0.4 degrees latitude and longitude spatially.
235 There could be multiple CATS retrievals corresponding to one CALIOP data point, and vice
236 versa. Thus, the collocated pairs are further averaged in such a way that only one pair of
237 collocated CATS and CALIOP data is derived for each collocation incident.

238 Figure 3a shows the comparison of CATS and CALIOP AODs for all collocated pairs
239 including both day- and night-time. A reasonable correlation of 0.7, with a slope of 0.69, is
240 found for a total of 2681 collocated data pairs. Further breaking down the comparison into day
241 and night cases, a much better agreement is found between the two datasets during nighttime
242 with a correlation of 0.84 and 0.81 for over-ocean and over-land cases respectively. In
243 comparison, a lower correlation of 0.62 (0.52), with a slope of 0.44 (0.63), is found between the
244 two datasets, using over land (ocean) daytime data only, for a total of 171 (1207) collocated
245 pairs. This result is not surprising as daytime data from both CALIOP and CATS are expected to
246 be nosier due to solar contamination (e.g. Omar et al., 2013; Toth et al., 2016).

247 Still, larger discrepancies between CATS and CALIOP AODs during daytime indicate
248 that both sensors are more susceptible to solar contamination. To overcome solar contamination
249 and more accurately detect aerosol layers, CALIOP and CATS data products are averaged up to
250 80 km and 60 km, respectively. Noel et al. (2018) found that clouds screened using the feature

type score were accurately detected by CATS data products throughout the diurnal envelope of solar angles. To ensure the solar contamination does not introduce a diurnal bias in aerosol detection or products, CATS AODs are further evaluated as a function of local time. For each CATS observation of a given location and UTC time, the associated local time is computed by adding (subtracting) the UTC time by 1 hour per 15° Longitude away from the Prime Meridian in the east (west) direction. Figure 4a shows the CATS AOD versus local time for both global land and oceans. While noisy in data, an averaged AOD peak is found around local noon that is about 0.02-0.03 higher than both sunrise and sunset times. Still, for high AOD cases, no significant solar noon peak is found. Also, no major deviations in AODs are found during either sunrise or sunset time, although it is speculated that larger uncertainties in CATS AODs and extinctions may be presented around day and night terminators. Figure 4b shows a similar plot as Figure 4a, but with the region restricted to 25°S-52°S. Here, we want to investigate the variations in CATS AODs as a function of local time, over relatively aerosol free oceans. We picked 25°S as the cutoff line as CATS data only available to 51.6°S (limited to the ISS inclination angle) and thus, this threshold is used to ensure enough data samples in the analysis, although some land regions are also included. As indicated in Figure 4b, a clear diurnal variation is found, with the peak mean AOD of 0.08 found around local noon and smaller AOD values of 0.06 found for both sunrise and sunset times. Also, no significant deviations in pattern are found for both sunrise and sunset time, plausibly indicating that solar contamination, as speculated, may not be as significant. It is, however, unclear if the 0.02 AOD difference between local noon and sunrise and sunset times is introduced by retrieval bias or indeed a physical existence.

To further explore the 0.02 difference, Figure 4c shows the difference between AERONET (1020 nm) and CATS (1064 nm) AOD (ΔAOD) as a function of local time, again,

although data are rather noisy, no major pattern is found near sunrise or sunset times, again, further indicating that solar contamination during dawn or dusk times, may have a less severe impact to CATS AOD retrievals from a long term mean perspective.

In summary, Sections 3.1.1-3.1.3 suggest that with careful QA procedures, AOD retrievals from CATS are comparable to those from other existing sensors such as AERONET, MODIS, and CALIOP at the same local times.

3.1.4 CATS-CALIOP Vertical Extinction Profiles

One advantage of CATS is its ability to retrieve both column-integrated AOD and vertical distributions of aerosol extinction. Therefore, in this section, extinction profiles from CATS are compared with that from CALIOP. Again, similar to the Section 3.1.3, collocated profiles for CATS and CALIOP are first found for both retrievals that are close in space and time (within ±30 minutes and 0.4 degrees latitude and longitude). However, different from Section 3.1.3, only one pair of collocated CATS and CALIOP profiles, which has the closest Euclidian distance on the earth's surface, is retained for each collocated incident.

The CATS cloud-aerosol discrimination (CAD) algorithm is a multidimensional probability density function (PDF) technique that is based on the CALIPSO algorithm (Liu et al. 2009). The PDFs were developed based on Cloud Physics Lidar (CPL) measurements obtained during over 11 field campaigns and 10 years. Figure 5 shows that CATS V2-01 aerosol extinction agrees very well with CALIOP for nighttime (Figure 5c) and over land (Figure 5e). However, CATS overestimates aerosol extinction around 1 km compared to CALIOP during daytime (Figure 5b) and over ocean (Figure 5d). Based on statistical comparisons of CATS L2O V2-01 cloud and aerosol detection frequencies with CALIOP, it was determined that, during

daytime over ocean, depolarizing liquid water clouds in the lower troposphere are sometimes classified as lofted dust mixture or smoke aerosols in the CATS V2-01 data products. This is primarily a result of enhanced depolarization ratios within liquid water clouds due to multiple scattering (which is not represented in the CPL measurements used for the PDFs). To overcome this issue, the CATS V3-00 CAD algorithm uses horizontal persistence tests and additional tests using variables such as the perpendicular ATB, to better differentiate clouds and aerosols. More details will be provided in an upcoming paper (Yorks et al., in prep). Since the CATS V3-00 data has not been released yet, we will focus our discussion of aerosol diurnal variability on regions primarily over land.

CATS also has a stronger extinction when compared to CALIOP in the lowest 2 km, which may be due to differences in cloud screening. Vertical profiles of collocated CATS and CALIOP extinction for daytime only profiles and nighttime only profiles are shown in Figure 5b and 5c, respectively. Compared to a total collocated pair count of 2681 in the overall profile data, day and night profiles have 1342 and 1339 collocated pairs, respectively. Again, the shapes of the CATS and the CALIOP nm extinction vertical profile are very similar for all three cases, despite the above mentioned offsets in altitude. Figure 5d and 5e show the mean of those extinction profiles which occurred over-water and over-land, as defined by the CATS surface type flag. Again in both cases CATS and CALIOP have very similar shapes in their vertical extinction profiles. The vertical structure of over-water extinction is also very similar to that of all profiles, day, and night, which is perhaps not surprising as water profiles made up 2111 of 2681 (~79%) collocated pairs. The vertical structure of over-land is more different than the other groups, as the extinction is higher throughout a larger depth of the atmosphere, tapering off much

more slowly from the surface. Furthermore, the extinction from CATS is actually lower than CALIOP for over-land profiles, unlike all other categories.

3.2 Diurnal Cycle of AODs and Aerosol Vertical Distributions

Using the QAed CATS data, seasonal variations as well as diurnal variations in CATS AODs are derived in this section. Diurnal variations in the vertical distributions of CATS aerosol extinction are also examined at both global and regional scales.

3.2.1 Seasonal and Diurnal Variation of AOD

Figures 6a-b show the spatial distributions of CATS AODs at the 1064 nm spectral channel for boreal winter-spring (Dec.-May, DJFMAM) and boreal summer-fall (June-Nov, JJASON) seasons, for the period of Feb. 2015-Oct. 2017. To construct Figures 6a and 6b, quality-assured CATS AODs are first binned on a 5 degree by 5 degree grid over the globe for the above mentioned two bi-seasons. For each 5×5° (Latitude/Longitude) bin, for a given season, CATS AODs are averaged on a pass-basis first, and then further averaged seasonally to represent AOD value of the given bin.

In DJFMAM season, significant aerosol features are found over North Africa, Mid-East, India and Eastern China. For the JJASON season, besides the above mentioned regions, aerosol plumes are also observable over Southern Africa, related to summer biomass burning of the region (e.g. Eck et al., 2013). The seasonal-based spatial distributions of AODs from CATS, although reported at the 1064 nm channel which is different from the 550 nm channel that is conventionally used, are similar to some published results (e.g. Lynch et al., 2016).

For comparison purposes, Figures 6c-6d shows similar plots as Figures 6a-6b, but with the use of CALIOP AOD at the 1064 nm spectral channel. Note that those are climatological means rather than pairwise comparisons. While patterns are similar in general, at regions with peak AODs of 0.4 or above for CALIOP, such as North Africa for the DJFMAM season and North Africa, Middle-East and India for the JJASON, much lower AODs are found for CATS. In some other regions, such as over South Africa and upper-portion of Middle-East for the JJASON season, however, higher CATS AOD values are observed. Figures 6e and 6f show the similar spatial plots as Figures 6a and 6b but with the use of Aqua MODIS AODs from the DT products. For the Aqua MODIS DT products, aerosol retrievals at the short-wave Infra-red channels are only available over oceans, and thus Figures 6e-6f show only over ocean retrievals. Again, while general AOD patters look similar, discrepancies are also visible, such as over the coast of south east Africa for the JJASON season. Those discrepancies may result from biases in each product, but it is also possibly due to the differences in satellite overpass times, as both MODIS and CALIOP provide early morning and afternoon over passes while CATS is able to report atmospheric aerosol distributions at multiple times during a day. It is also possibly due to aerosol above cloud related issues as reported by Rajapakshe et al. (2017).

Similar to Figures 6a and 6b, Figures 7a and 7b show the spatial distribution of CATS AODs, but for CATS extinction values that are below 1 km AGL only, for the DJFMAM and JJASON seasons respectively. Figure 7c and 7d (7e and 7f) show the CATS mean AOD plots for extinction values from 1-2 km AGL (> 2 km AGL). For the DJFMAM season, elevated aerosol plumes with altitude above 2 km AGL are found over the North coast of Africa. For the JJASON season, elevated dust plumes (> 2 km AGL) are found over North Africa and the Middle-East regions, while elevated smoke plumes are found over the west coast of South Africa

Atmos. Chem. Phys. Discuss., https://doi.org/10.5194/acp-2018-1298
Manuscript under review for journal Atmos. Chem. Phys.
Discussion started: 20 December 2018

where above cloud smoke plumes are often observed during the Northern hemispheric summer season (e.g. Alfaro-Contreras et al., 2016).

CATS has a non-sun-synchronized orbit, which enables measurements at near all solar angles. Thus, we also constructed 5×5° (Latitude/Longitude) gridded seasonal averages (for DJFMAM and JJASON seasons) of CATS AODs at 0, 6, 12 and 18 UTC that represent 4 distinct times in a full diurnal cycle, as shown in Figure 8. To construct the seasonal averages, observations within ±3 hours of a given UTC time as mentioned above are averaged to represent AODs for the given UTC time. On a global average, the mean AODs are 0.090, 0.090, 0.090 and 0.091 for 0, 6, 12 and 18 UTC respectively for the JJASON season and are 0.101, 0.100, 0.097 and 0.097 for the DJFMAM season. Thus, no significant diurnal variations are found on a global scale, as global means are dominated by background aerosols that have weak diurnal variations in measured absolute AOD values.

Still, strong diurnal variations with the maximum averaged diurnal AOD changes of above 0.15 can be observed for regions with significant aerosol events such as Northern Africa and India for the DJFMAM season and Northern Africa, Southern Africa, Mid-East and India for the JJASON season, as illustrated in Figure 9. Note that Fig. 9a (9b) shows the maximum minus minimum seasonal mean AODs for the four difference times as shown in Figs. 8a,c,e,g (8b,d,f,h). Interestingly but not unexpectedly, regions with maximum diurnal variations match well with locations of heavy aerosol plumes as shown in Figures 6 and 8.

3.2.2 Diurnal variations of Aerosol Extinction on a Global Scale (both at UTC and local time)

Using quality-assured CATS derived aerosol vertical distributions, mean global CATS extinction vertical profiles are also generated as shown in Figure 10. Similar to steps as described in the section 3.2.1, CATS extinction profiles are binned into 00, 06, 12, and 18 UTC times based on the closest match in time for the JJASON and DJFMAM seasons. Figure 10a (10d) shows the daily averaged CATS extinction profiles in a black line, and 00, 06, 12 and 18 UTC averaged in blue, green, yellow and red lines respectively, for the DJFMAM (JJASON) season. CATS extinction profiles for the daily average as well averages for the four selected times are similar, suggesting that minor temporal variations in CATS extinctions can be expected for global averages.

Those global averages are dominated by CATS profiles from global oceans (Figure 10b and 10e), which also have small diurnal variations, as ~70% of the globe is covered by water. In comparison, noticeable diurnal changes in aerosol vertical distributions are found over land as shown in Figure 10c and 10f. For the DJFMAM season, at the 1 km altitude, the minimum and maximum aerosol extinctions are at 12 and 18 UTC respectively. Similarly, the minimum and maximum aerosol extinctions are at 18 and 6 UTC at the altitude of 400 m. For the JJASON season, the minimum aerosol extinction values are found at 12 UTC for the whole 0-2 km column, while the maximum aerosol extinction values are at 18UTC for 1.5 km and 0UTC for the 300-400 m altitude. Still, it should be noted that aerosol concentrations may be a function of local time, yet for a given UTC time, local times will vary by region. Also, due to solar contamination, nighttime retrievals from CATS are considered to be less noisy than daytime retrievals, and this difference in sensor sensitivity between day and night may further affect the derived diurnal variations in CATS AOD and aerosol vertical profiles as shown in Figure 3 for individual retrievals. Still, no apparent solar pattern is detectable from Figure 8, and only minor

diurnal variations are found for Figure 10a and 10d, which indicate that such a solar contamination may introduce noise but not bias to daytime aerosol retrievals, from a global mean perspective.

If we examine the mean global CATS extinction vertical profiles with respect to local time as shown in Figure 11, however, some distinct features appear. For example, Figure 11a and 11d suggests that on global average, the minimum and maximum aerosol extinction below 1 km is found for 6:00 pm and 12:00 pm local time, respectively for both JJASON and DJFMAM seasons. Similar patterns are also observed for over global oceans. However, for over land cases, for both seasons, peak in aerosol extinction is found at the 500-1000 m layer for local noon, which is ~20-30% higher than daily mean values. This may indicate stronger solar heating at the surface and hence stronger near surface convection at local noon that brings near surface aerosol particles to a higher altitude.

3.2.3 Diurnal variations of Aerosol Extinction on a Regional Scale (at local time)

In this section, the diurnal variations of aerosol vertical distributions are studied as a function of local solar time for selected regions with high mean AODs as highlighted in Figure 6. We picked local solar time here as for those regional analyses, near 1 to 1 transformation can be achieved between UTC and local solar time. Also, as learned from the previous section, aerosol features are likely to have a local time dependency. A total of four regions, including Africa-north, Middle East, India and Northeast China, which show significant season all mean AODs in Figure 6, are selected for the DJFMAM season (Figure 12). For the JJASON season (Figure 13), in addition to the above mentioned 4 regions, the Africa-south region is also included due to biomass burning in the region during the Northern Hemisphere summer time. The

Latitude/Longitude boundary of each selected region is described in Table 1. Regional-based analyses are also conducted for 4 (5) selected regions for the DJFMAM (JJASON) season at four local times: 0:00 am, 6:00 am, 12:00 pm and 6:00 pm, using quality assured CATS profiles. Generally, the maximum diurnal change in aerosol extinction is found at the altitude of below 1 km for all regions as well for both seasons. Also, larger diurnal variations in vertical distributions of aerosol extinction are found for the JJASON season, in-comparing with the DJFMAM season, while regional-based differences are apparent.

For the Africa-north region, dominant aerosol types are dust and smoke aerosol for the DJFMAM season, and is dust for the JJASON season (e.g. Remer et al., 2008). Interestingly, the maximum aerosol extinction below 500m is found at 6:00 am for the DJFMAM season. While for the JJASON season, the maximum aerosol extinctions are found at 6:00 am for the whole 0-2 km column, with a significant ~20% higher aerosol extinction from either daily mean or vertical profiles from 0:00 am, 12:00 pm and 6:00 pm. Note that 6:00 am in the Africa-north region corresponds to early morning, which has been identified in several studies (Fiedler et al., 2013; Ryder et al. 2015) as the time of day when nocturnal low-level jet breakdown causes large amounts of dust emission in this region. Thus, we suspect that this large 6:00 am peak in maximum aerosol extinctions may be the signal resulting from the low-level jet ejection mechanism captured on a regional scale. As the day progresses into the afternoon and early evening, we find the aerosol heights shifting upwards, likely related to the boundary layer's mixed layer development.

For the Middle East region, for the JJASON season, a daily maximum in aerosol extinction of ~0.13 km^{-1} is found at local morning or early morning (0:00 am and 6:00 am) , with a daily minimum of ~0.09 km^{-1} found at local noon (12:00 pm), for the peak aerosol extinction

455 layer that has a daily mean aerosol extinction of ~~0.11 km^{-1}. This translates to a ~±20% daily
456 variation for aerosol extinction for the peak aerosol extinction layer. Much smaller daily
457 variation in aerosol extinction, however, is found for the same region for the DJFMAM season.
458 For the India region, for the JJASON season, a large peak in aerosol extinction of up to
459 20% higher than daily mean is found at 6:00 am below 1 km. The minimum aerosol extinction is
460 found at 0:00 am for the layer of ~400-1000 m, and is overall ~10% lower than the daily means.
461 The minimum aerosol extinction is found at 6:00 pm for the layer below 400 m. For the
462 DJFMAM season, minimum aerosol extinctions are found at 12:00 pm for near the whole 0-2 km
463 column, while for the layer below 500 m, the maximum aerosol extinction values are found at
464 early morning (0:00 am and 6:00 am). This is consistent with the diurnal formation of
465 significant haze.
466 For the Northeast China region, less diurnal variation is found for the DJFMAM season.
467 Yet, a significant peak found at 1km for local noon (12:00 pm) for the JJASON season, which is
468 ~30% higher than daily averages for the JJASON season. The reason for this elevated peak at
469 regional local noon, however, is not known, although it may relate to the peak in surface
470 Particulate Matter concentrations. Lastly, for the Africa-south region, biomass burning aerosols
471 are prevalent during the summer time and thus only the JJASON season is analyzed. As shown
472 in 13b, below 500m in altitude, lower extinction values are found for local afternoon (12:00 pm
473 and 6:00 pm) and higher extinction values are found for local morning or early morning (0:00
474 and 6:00 am). Still, the diurnal variation in aerosol vertical distribution is rather marginally for
475 the region.
476

477 **4.0 Conclusions**

Using CALIOP, MODIS and AERONET data, we evaluated CATS derived AODs as well as vertical distributions of aerosol extinctions for the study period of for Feb. 2015 – Oct. 2017. CATS data (at 1064 nm) are further used to study variations in AODs and aerosol vertical distributions diurnally. We found:

(1) Quality assurance steps are critical for applying CATS data in aerosol related applications. With a 10% data loss due to QA steps, an improvement in correlation from 0.17 to 0.64 is found for the collocated CATS and AERONET AOD comparisons. Using quality assured CATS data, reasonable agreements are found between CATS derived AODs and AODs from CALIOP, Aqua MODIS DT and Terra MODIS DT at the same local times, with correlations of 0.70, 0.75 and 0.71 respectively.

(2) While the averaged vertical distributions from CATS compare reasonably well with that from CALIOP, differences in peak extinction altitudes are present. This may due to contamination of daytime aerosol detections over ocean by marine boundary layer clouds in the CATS V2-01 data products, which will hopefully be resolved in the future CATS V3-00 data.

(3) From the global mean perspective, minor changes are found for AODs at four selected times, namely 00, 06, 12 and 18 UTC. Yet noticeable diurnal variations in AODs of above 0.15 (at 1064 nm) are found for regions with extensive aerosol events, such as over North Africa, and India for the DJFMAM season, and over North and South of Africa, India and Middle East for the JJASON season.

(4) From the global mean perspective, changes are less noticeable for the averaged aerosol extinction profiles at 00, 06, 12 and 18 UTC. Yet, if the study is repeated

with respect to local time, a peak in aerosol extinction is found for local noon and the minimum value in aerosol extinction is found at 6:00 pm local time for both JJASON and DJFMAM seasons. In particular, for over land cases, in both seasons, a lifted aerosol plume at 500-1000 m altitude (with the peak aerosol extinction that is ~20-30% higher that daily averages) is found at local noon, which may indicate the impact of strong surface solar heating as well as stronger near surface convection on aerosol vertical distributions.

(5) Larger diurnal variations are found at regions with heavy aerosol plumes such as North and South (summer season only) of Africa, Middle East, India and Eastern China. In particular, aerosol extinctions from 6:00 am over North Africa are ~20% higher than daily means as well other three times for the 0-2 km column for the JJASON season. We suspect this may be related to increase in dust concentrations due to breakdown of low level jets at early morning time for the region.

This paper suggests that strong regional diurnal variations exist for both AOD and aerosol extinction profiles. These results demonstrate the need for global aerosol measurements throughout the entire diurnal cycle to improve visibility and particulate matter forecasts as well as studies focused on aerosol climate applications.

Author Contribution:

Authors J. Zhang, J. S. Reid and L. Lee designed the study. L. lee worked on data processing for the project. J. E. Yorks guided L. lee on data processing. The manuscript was written with inputs from all coauthors.

Acknowledgments:

We acknowledge the support of ONR grant (N00014-16-1-2040) and NASA grant (NNX17AG52G) for this study. L. Lee is also partially supported by the NASA NESSF fellowship grant (NNX16A066H). J. S Reid's participation was supported by the Office of Naval Research Code 322 and 33. We thank the NASA AERONET team for the AERONET data used in this study.

References:

Aerosol Product Application Team of the AWG Aerosols/Air Quality/Atmospheric Chemistry Team: GOES-R Advanced Baseline Imager (ABI) algorithm theoretical basis document for suspended matter/aerosol optical depth and aerosol size parameter, NOAA/NESDIS/STAR July 2012, https://www.star.nesdis.noaa.gov/goesr/docs/ATBD/AOD.pdf (last accessed on Nov. 17, 2018).

Alfaro-Contreras, R., Zhang, J., Campbell, J. R., and Reid, J. S.: Investigating the frequency and trends in global above-cloud aerosol characteristics with CALIOP and OMI, Atmos. Chem. Phys., 16, 47-69, doi:10.5194/acp-16-47-2016, 2016.

Campbell, J. R., Tackett, J. L., Reid, J. S., Zhang, J., Curtis, C. A., Hyer, E. J., Sessions, W. R., Westphal, D. L., Prospero, J. M., Welton, E. J., Omar, A. H., Vaughan, M. A., and Winker, D. M.: Evaluating nighttime CALIOP 0.532 μm aerosol optical depth and extinction coefficient retrievals, Atmos. Meas. Tech., 5, 2143-2160, https://doi.org/10.5194/amt-5-2143-2012, 2012.

Christopher, S. A. and Zhang, J.: Daytime variation of shortwave direct radiative forcing of biomass burning aerosols from GOES 8 imager, J. Atmos. Sci., 59, 681–691, 2002.

Eck, T .F., Holben, B. N., Reid, J. S., Mukelabai, M. M., Piketh, S. J., Torres, O., Jethva, H. T., Hyer, E. J., Ward, D. E., Dubovik, O., and Sinyuk, A.: A seasonal trend of single scattering albedo in southern African biomass-burning particles: Implications for satellite products and estimates of emissions for the world's largest biomass-burning source, J. Geophys. Res.-Atmos., 118, 6414–6432, 2013.

552 Fiedler, S., Schepanski, K., Heinold, B., Knippertz, P., and Tegen, I.: Climatology of
553 nocturnal low-level jets over North Africa and implications for modeling mineral dust
554 emission, J. Geophys. Res. Atmos., 118, 6100–6121, doi: 10.1002/jgrd.50394, 2013.
555 Giglio, L., Kendall, J.D., Mack, R.: A multi-year active fire dataset for the tropics derived
556 from the TRMM VIRS,. International Journal of Remote Sensing 24, 4505-4525, 2003.
557 Giles, D. M., Sinyuk, A., Sorokin, M. S., Schafer, J. S., Smirnov, A., Slutsker, I., Eck, T. F.,
558 Holben, B. N., Lewis, J., Campbell, J., Welton, E. J., Korkin, S., and Lyapustin, A.:
559 Advancements in the Aerosol Robotic Network (AERONET) Version 3 Database –
560 Automated Near Real-Time Quality Control Algorithm with Improved Cloud Screening
561 for Sun Photometer Aerosol Optical Depth (AOD) Measurements, Atmos. Meas. Tech.
562 Discuss., https://doi.org/10.5194/amt-2018-272, in review, 2018.
563 Heinold, B., Knippertz, P., Marsham, J. H., Fiedler, S., Dixon, N. S., Schepanski, K.,
564 Laurent, B., and Tegen, I.: The role of deep convection and nocturnal low-level jets for
565 dust emission in summertime West Africa: Estimates from convection-permitting
566 simulations, J. Geophys. Res. Atmos., 118, 4385–4400, doi:10.1002/jgrd.50402, 2013.
567 Holben, B. N., and coauthors: AERONET—A Federated Instrument Network and Data
568 Archive for Aerosol Characterization. Remote Sensing of Environment, 66(1), 1–16.
569 https://doi.org/10.1016/S0034-4257(98)00031-5, 1998.
570 Hyer, E. J., Reid, J. S., Prins, E. M., Hoffman, J. P., Schmidt, C. C., Miettinen, J. I., and
571 Giglio, L.: Different views of fire activity over Indonesia and Malaysia from polar and
572 geostationary satellite observations, *Atmos. Res.*, 122, 504-519, 2013.
573 Kaku K. C., Reid, J. S., Hand, J. L., Edgerton, E. S., Holben, B. N., Zhang, J., and Holz, R.
574 E.: Assessing the challenges of surface-level aerosol mass estimates from remote sensing

during the SEAC4RS campaign: Baseline surface observations and remote sensing in the Southeastern United States, JGR, doi: 10.1029/2017JD028074, 2018.

Levy, R. C., Mattoo, S., Munchak, L. A., Remer, L. A., Sayer, A. M., Patadia, F., and Hsu, N. C.: The Collection 6 MODIS aerosol products over land and ocean. Atmos. Meas. Tech., 6(11), 2989–3034. https://doi.org/10.5194/amt-6-2989-2013, 2013.

Liu, Z., and coauthors: The CALIPSO Lidar Cloud and Aerosol Discrimination: Version 2 Algorithm and Initial Assessment of Performance, *J. Atmos. Oceanic Technol.*, 26, 1198–1213, 2009.

Lynch, P., Reid, J. S., Westphal, D. L., Zhang, J., Hogan, T. F., Hyer, E. J., Curtis, C. A., Hegg, D. A., Shi, Y., Campbell, J. R., Rubin, J. I., Sessions, W. R., Turk, F. J., and Walker, A. L.: An 11-year global gridded aerosol optical thickness reanalysis (v1.0) for atmospheric and climate sciences, Geosci. Model Dev., 9, 1489-1522, https://doi.org/10.5194/gmd-9-1489-2016, 2016.

Mbourou, G. N., Berand, J. J., and Nicholson, S. E.: The diurnal and seasonal cycle of wind-borne dust over Africa north of the equator, J. Appl. Meteor., 36, 868-882, 1997.

McGill, M. J., Yorks, J. E., Scott, V. S., Kupchock, A. W., and Selmer, P. A.: The Cloud-Aerosol Transport System (CATS): A technology demonstration on the International Space Station, Proc. SPIE 9612, Lidar Remote Sensing for Environmental Monitoring XV, 96120A, doi:10.1117/12.2190841, 2015.

Noel, V., Chepfer, H., Chiriaco, M., and Yorks J. E.: The diurnal cycle of cloud profiles over land and ocean between 51° S and 51° N, seen by the CATS spaceborne lidar from the International Space Station, Atmos. Chem. Phys., 18, 9457-9473, https://doi.org/10.5194/acp-18-9457-2018, 2018.

598 Omar, A. H., Winker, D. M., Tackett, J. L., Giles, D. M., Kar, J., Liu, Z., Vaughan, M. A.,
599 Powell, K. A., and Trepte C. R.: CALIOP and AERONET aerosol optical depth
600 comparisons: One size fits none, J. Geophys. Res. Atmos., 118, 4748–4766, doi:
601 10.1002/jgrd.50330, 2013.
602 Rajapakshe, C., Zhang, Z., Yorks, J. E., Yu, H., Tan, Q., Meyer, K., Platnick, S.: Seasonally
603 Transported Aerosol Layers over Southeast Atlantic are Closer to Underlying Clouds
604 than Previously Reported, Geophys. Res. Lett., 44, doi:10.1002/2017GL073559, 2017.
605 Redemann, J., Vaughan, M. A., Zhang, Q., Shinozuka, Y., Russell, P. B., Livingston, J. M.,
606 … Remer, L. A.: The comparison of MODIS-Aqua (C5) and CALIOP (V2 & V3) aerosol
607 optical depth. Atmospheric Chemistry and Physics, 12(6), 3025–3043.
608 https://doi.org/https://doi.org/10.5194/acp-12-3025-2012, 2012.
609 Reid, J.S., Eck, T. F., Christopher, S. A., Hobbs, P. V., and Holben B. R.: Use of the
610 Angstrom exponent to estimate the variability of optical and physical properties of aging
611 smoke particles in Brazil, J. Geophys. Res., *104*, 27,489-27,489, 1999.
612 Remer, L. A., and coauthors: Global aerosol climatology from the MODIS satellite sensors,
613 J. Geophys. Res., 113, D14S07, doi: 10.1029/2007JD009661, 2008.
614 Ryder, C. L., McQuaid, J. B., Flamant, C., Rosenberg, P. D., Washington, R., Brindley, H.
615 E., Highwood, E. J., Marsham, J. H., Parker, D. J., Todd, M. C., Banks, J. R., Brooke, J.
616 K., Engelstaedter, S., Estelles, V., Formenti, P., Garcia-Carreras, L., Kocha, C., Marenco,
617 F., Sodemann, H., Allen, C. J. T., Bourdon, A., Bart, M., Cavazos-Guerra, C.,
618 Chevaillier, S., Crosier, J., Darbyshire, E., Dean, A. R., Dorsey, J. R., Kent, J.,
619 O'Sullivan, D., Schepanski, K., Szpek, K., Trembath, J., and Woolley, A.: Advances in
620 understanding mineral dust and boundary layer processes over the Sahara from Fennec

aircraft observations, Atmos. Chem. Phys., 15, 8479-8520, https://doi.org/10.5194/acp-15-8479-2015, 2015.

Shi Y., Zhang, J., Reid, J. S., Hyer, E., and Hsu, N. C.: Critical evaluation of the MODIS Deep Blue aerosol optical depth product for data assimilation over North Africa, Atmos. Meas. Tech., 6, 949-969, doi:10.5194/amt-6-949-2013, 2013.

Shi Y., Zhang J., Reid J. S., Hyer E. J., Eck T. F., and Holben B. N.: A critical examination of spatial biases between MODIS and MISR aerosol products – application for potential AERONET deployment, Atmos. Meas. Tech., 4, 2823–2836, 2011.

Stephens, G. L., and coauthors: The CLOUDSAT mission and the A-TRAIN, Bulletin of the American Meteorological Society, 83(12), 1771–1790. https://doi.org/10.1175/BAMS-83-12-1771, 2002.

Tiwari, S., Srivastava, A. K., Bisht, D. S., Parmita, P., Srivastava, M. K., and Atri, S. D.: Diurnal and seasonal variaition of black carbon and PM2.5 over New Delhi, india: Influence of meteorology, Atmos. Res, 125, 50-62, doi:10.1016/j.atmos.res.2013.01.011, 2013.

Toth, T. D., Campbell, J. R., Reid, J. S., Tackett, J. L., Vaughan, M. A., Zhang, J., & Marquis, J. W.: Minimum aerosol layer detection sensitivities and their subsequent impacts on aerosol optical thickness retrievals in CALIPSO level 2 data products. Atmospheric Measurement Techniques, 11(1), 499–514. https://doi.org/https://doi.org/10.5194/amt-11-499-2018, 2018.

Toth, T. D., Zhang, J., Campbell, J. R., Reid, J. S., & Vaughan, M. A.: Temporal variability of aerosol optical thickness vertical distribution observed from CALIOP, Journal of

643 Geophysical Research: Atmospheres, 121(15), 9117–9139.
644 https://doi.org/10.1002/2015JD024668, 2016.
645 Vaughan, M., Garnier, A., Josset, D., Avery, M., Lee, K.-P., Liu, Z., Hunt, W., Pelon, J.,
646 Tackett, J., Getzewich, B., Kar, J., and Burton, S.: CALIPSO Lidar Calibration at 1064
647 nm: Version 4 Algorithm, in preparation, 2018.
648 Wang, J., Liu, X., Christopher, S. A., Reid, J. S., Reid, E. A., and Maring, H.: The effects of
649 non-sphericity on geostationary satellite retrievals of dust aerosols, Geophys. Res. Lett.,
650 30(24), 2293, doi:10.1029/2003GL018697, 2003.
651 Winker, D. M., and coauthors: Overview of the CALIPSO Mission and CALIOP Data
652 Processing Algorithms. Journal of Atmospheric and Oceanic Technology, 26(11), 2310–
653 2323. https://doi.org/10.1175/2009JTECHA1281.1, 2009.
654 Yorks, J. E., McGill, M. J., Palm, S. P., Hlavka, D. L., Selmer, P. A., Nowottnick, E.,
655 Vaughan, M. A., Rodier, S., and Hart W. D.: An Overview of the CATS Level 1 Data
656 Products and Processing Algorithms, Geophys. Res. Let., 43,
657 doi:10.1002/2016GL068006., 2016.
658 Yorks, J. E., Rodier, S.D., Nowottnick, E., Selmer, P.A., McGill, M.J., Palm, S.P., and
659 Vaughan, M. A.: CATS Level 2 Vertical Feature Mask Algorithms and Data Products:
660 An Overview and Initial Assessment, Atmos. Meas. Tech. Discuss., in preparation.
661 Yoshida M., Kikuchi, M., Nagao, T. M., Murakami, H., Nomaki, T., and Higurashi, A.:
662 Common Retrieval of Aerosol Properties for Imaging Satellite Sensors, Journal of the
663 Meteorological Society of Japan. Ser. II, Article ID 2018-039, [Advance publication],
664 https://doi.org/10.2151/jmsj.2018-039, 2018.

665 Zhao, X. J., Zhang, X. L., Xu, X. F., Xu, J., Meng, W., and Pu, WW.: Seasonal and diurnal
666 variation of ambient PM2.5 concentrations in urban and rural environments in Beijing,
667 Atmos. Environ., 43, 2893-2900, doi: 10.106/j.atmosenv.2009.03.009., 2009.
668

Atmos. Chem. Phys. Discuss., https://doi.org/10.5194/acp-2018-1298
Manuscript under review for journal Atmos. Chem. Phys.
Discussion started: 20 December 2018

Table 1. Geographic ranges, height above ground level of maximum extinction, diurnal extinction range at height of maximum extinction, and time (local) of peak extinction for the boxed red regions in Figure 6 and vertical profiles shown in Figures 12 and 13.

			DJFMAM/JJASON		
Region	Latitude	Longitude	Height AGL (m) of Max. Extinction	Extinction Range (km^{-1}) at Height AGL of Max. Extinction	Time of Peak Extinction at Height AGL of Max. Extinction
India	7.5°N - 32.5°N	65°E - 85°E	180/240	0.109-0.131/0.138-0.182	6 am/6 am
Africa - North	2.5°N - 22.5°N	35°W - 20°E	420/480	0.107-0.130/0.098-0.121	12 pm/6 am
Africa - South	17.5°S - 2.5°N	0° - 30°E	/420	/0.090-0.100	/6 am
Middle East	12.5°N - 27.5°N	35°E - 50°E	240/180	0.093-0.116/0.081-0.135	6 am/0 am
China	27.5°N - 37.5°N	110°E - 120°E	240/240	0.107-0.154/0.085-0.133	6 am/6 am

673 **Figure Captions**
674
675 **Figure 1.** Collocated AERONET 1020 nm AOT vs. CATS 1064 nm AOD a) without CATS QA
676 applied, and b) with CATS QA applied.

677 **Figure 2.** Collocated MODIS C6.1 a) Terra and b) Aqua estimated 1064 nm AOD vs. CATS
678 1064 nm AOD with CATS QA applied.

679 **Figure 3.** Collocated CALIOP 1064 nm AOD vs. CATS 1064 nm AOD with CATS QA applied
680 for a) both day and night, b) nighttime over-land, c) nighttime over-water, d) daytime over-land,
681 e) daytime over-water.

682 **Figure 4:** CATS 1064 nm AOD a) as a function of local time for the globe, and b) as a function
683 of local time for areas south of -25 degrees. The difference between CATS 1064 nm AOD and
684 AERONET 1020 nm AOD as a function of local time is shown in c). The mean is represented
685 by the blue line, while the median is the green line.

686 **Figure 5.** CATS and CALIOP vertical profiles of 1064 nm extinction for a) all profiles, b)
687 daytime only, c) nighttime only, d) over-water, and e) over land.

688 **Figure 6.** Mean AOD (1064 nm) by season for a) DJFMAM CATS, b) JJASON CATS, c)
689 DJFMAM CALIOP, d) JJASON CALIOP, e) DJFMAM MODIS Aqua, and f) JJASON MODIS
690 Aqua. Red boxes indicate locations of regional vertical distributions in Figures 12 and 13.

691 **Figure 7.** Mean CATS AOD (1064 nm) by season for a) DJFMAM below 1 km AGL, b)
692 JJASON below 1 km AGL, c) DJFMAM 1-2 km AGL, d) JJASON 1-2 km AGL, e) DJFMAM
693 above 2 km AGL, and f) JJASON above 2 km AGL.

694 **Figure 8.** Seasonal Mean AOD (1064 nm) binned by every 6-hours for a) DJFMAM 0 UTC, b)
695 JJASON 0 UTC, c) DJFMAM 6 UTC, d) JJASON 6 UTC, e) DJFMAM 12 UTC, f) JJASON 12
696 UTC, g) DJFMAM 18 UTC, and h) JJASON 18 UTC.

697 **Figure 9.** Maximum minus minimum mean seasonal AOD (1064 nm) for a) DJFMAM, and b)
698 JJASON.

699 **Figure 10.** Global mean 6-hourly vertical profiles of CATS 1064 nm extinction for a) DJFMAM
700 all profiles, b) DJFMAM water profiles, c) DJFMAM not-water profiles, e) JJASON all profiles,
701 f) JJASON water profiles, g) JJASON not-water profiles.

702 **Figure 11.** Global mean 6-hourly local time (0:00 am, 6:00 am, 12:00 pm and 6:00 pm) vertical
703 profiles of CATS 1064 nm extinction for a) DJFMAM all profiles, b) DJFMAM water profiles,
704 c) DJFMAM not-water profiles, d) JJASON all profiles, e) JJASON water profiles, f) JJASON
705 not-water profiles.

706 **Figure 12.** DJFMAM 6-hourly average (local time; 0:00 am, 6:00 am, 12:00 pm and 6:00 pm)
707 vertical profiles of CATS 1064 nm for locations shown in Figure 6a; a) Africa-north, b) Middle
708 East, c) India, and d) Northeast China.

709

710 **Figure 13.** JJASON 6-hourly average (local time; 0:00 am, 6:00 am, 12:00 pm and 6:00 pm)
711 vertical profiles of CATS 1064 nm for locations shown in Figure 6b; a) Africa-north, b) Africa-
712 south, c) Middle East, d) India, and e) Northeast China.

713

714

715

Atmos. Chem. Phys. Discuss., https://doi.org/10.5194/acp-2018-1298
Manuscript under review for journal Atmos. Chem. Phys.
Discussion started: 20 December 2018

716

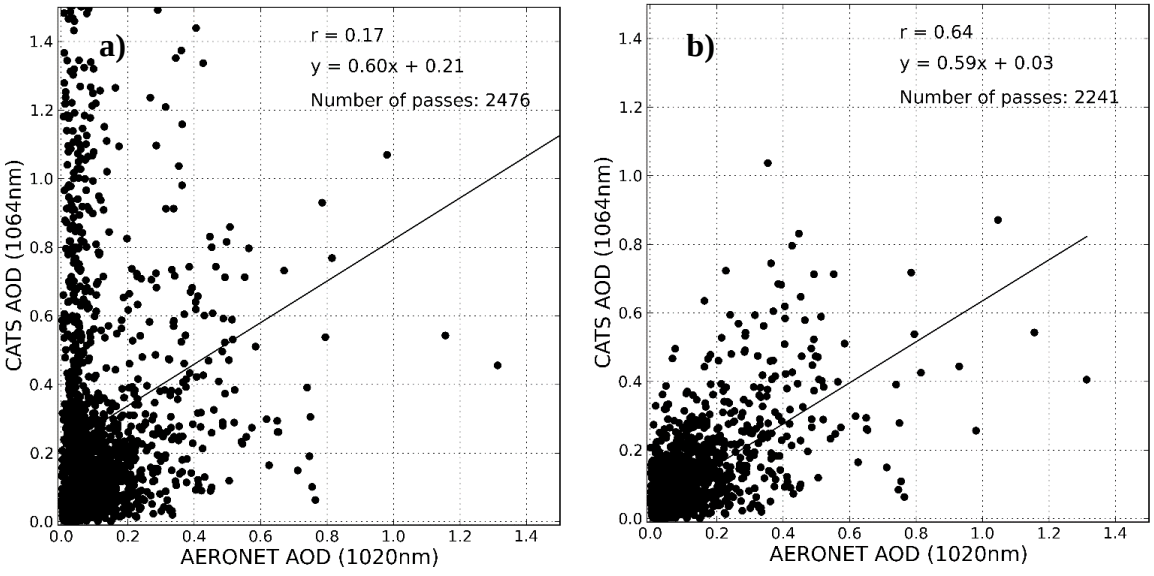

Figure 1. Collocated AERONET 1020 nm AOT vs. CATS 1064 nm AOD a) without CATS QA applied, and b) with CATS QA applied.

Atmos. Chem. Phys. Discuss., https://doi.org/10.5194/acp-2018-1298
Manuscript under review for journal Atmos. Chem. Phys.
Discussion started: 20 December 2018

717

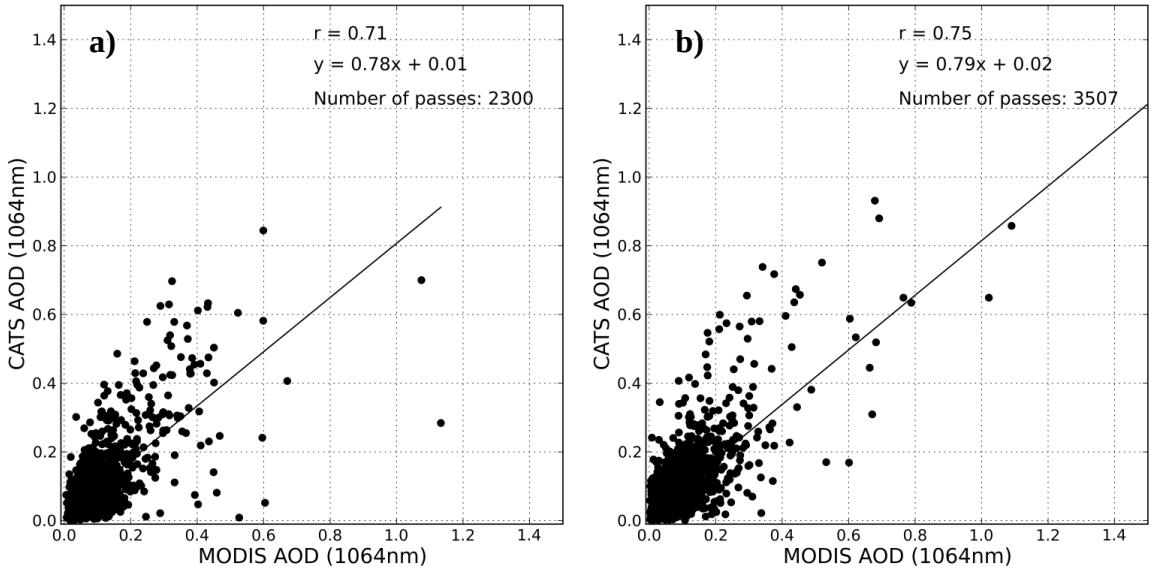

Figure 2. Collocated MODIS C6.1 a) Terra and b) Aqua estimated 1064 nm AOD vs. CATS 1064 nm AOD with CATS QA applied.

Atmos. Chem. Phys. Discuss., https://doi.org/10.5194/acp-2018-1298
Manuscript under review for journal Atmos. Chem. Phys.
Discussion started: 20 December 2018

718

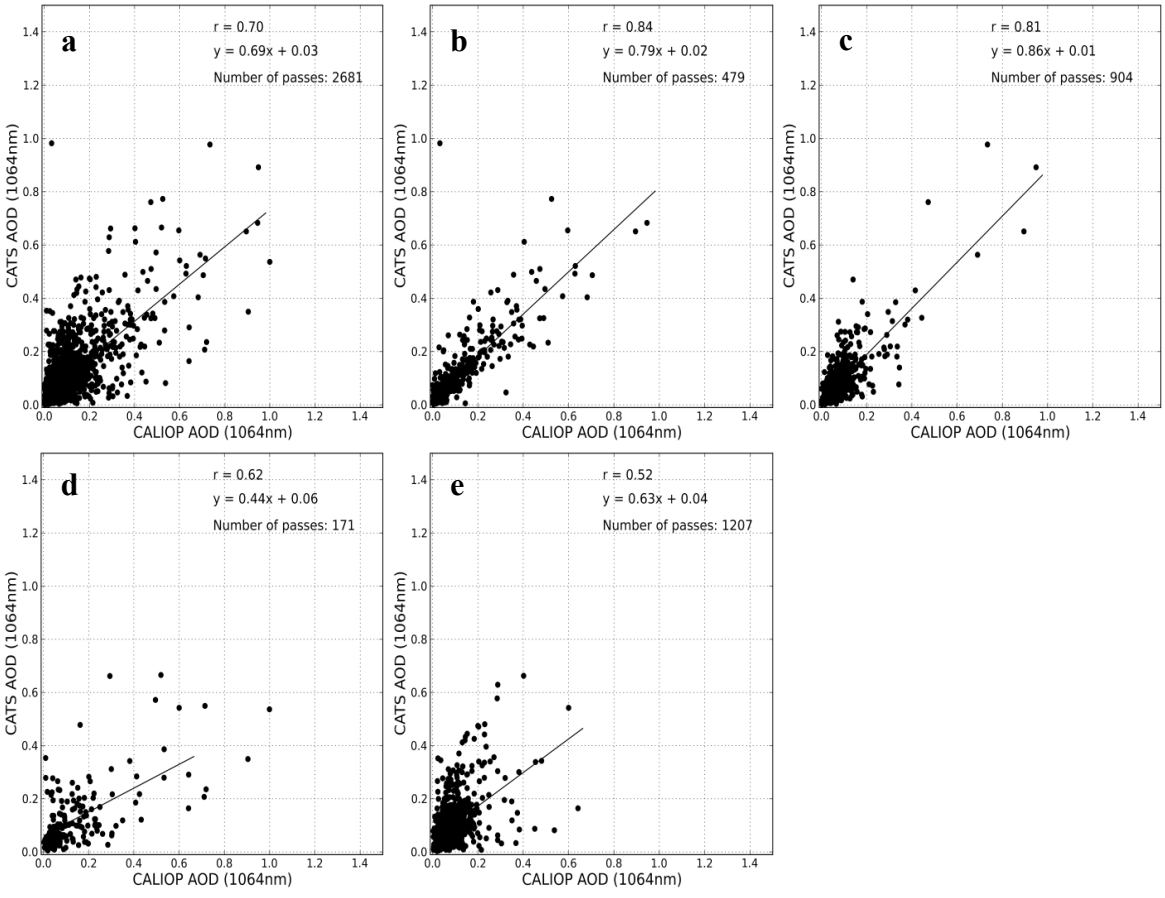

Figure 3. Collocated CALIOP 1064 nm AOD vs. CATS 1064 nm AOD with CATS QA applied for a) both day and night, b) nighttime over-land, c) nighttime over-water, d) daytime over-land, e) daytime over-water.

Atmos. Chem. Phys. Discuss., https://doi.org/10.5194/acp-2018-1298
Manuscript under review for journal Atmos. Chem. Phys.
Discussion started: 20 December 2018

719

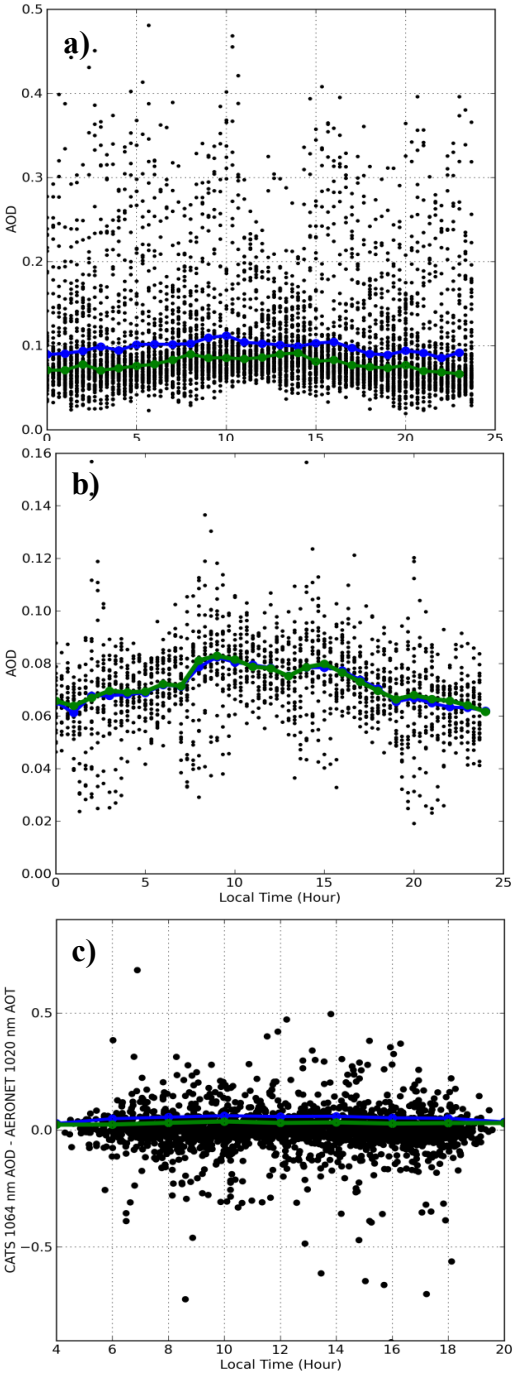

Figure 4: CATS 1064 nm AOD a) as a function of local time for the globe, and b) as a function of local time for areas south of -25 degrees. The difference between CATS 1064 nm AOD and AERONET 1020 nm AOD as a function of local time is shown in c). The mean is represented by the blue line, while the median is the green line.

Atmos. Chem. Phys. Discuss., https://doi.org/10.5194/acp-2018-1298
Manuscript under review for journal Atmos. Chem. Phys.
Discussion started: 20 December 2018

Atmospheric Chemistry and Physics Discussions

720
721
722
723

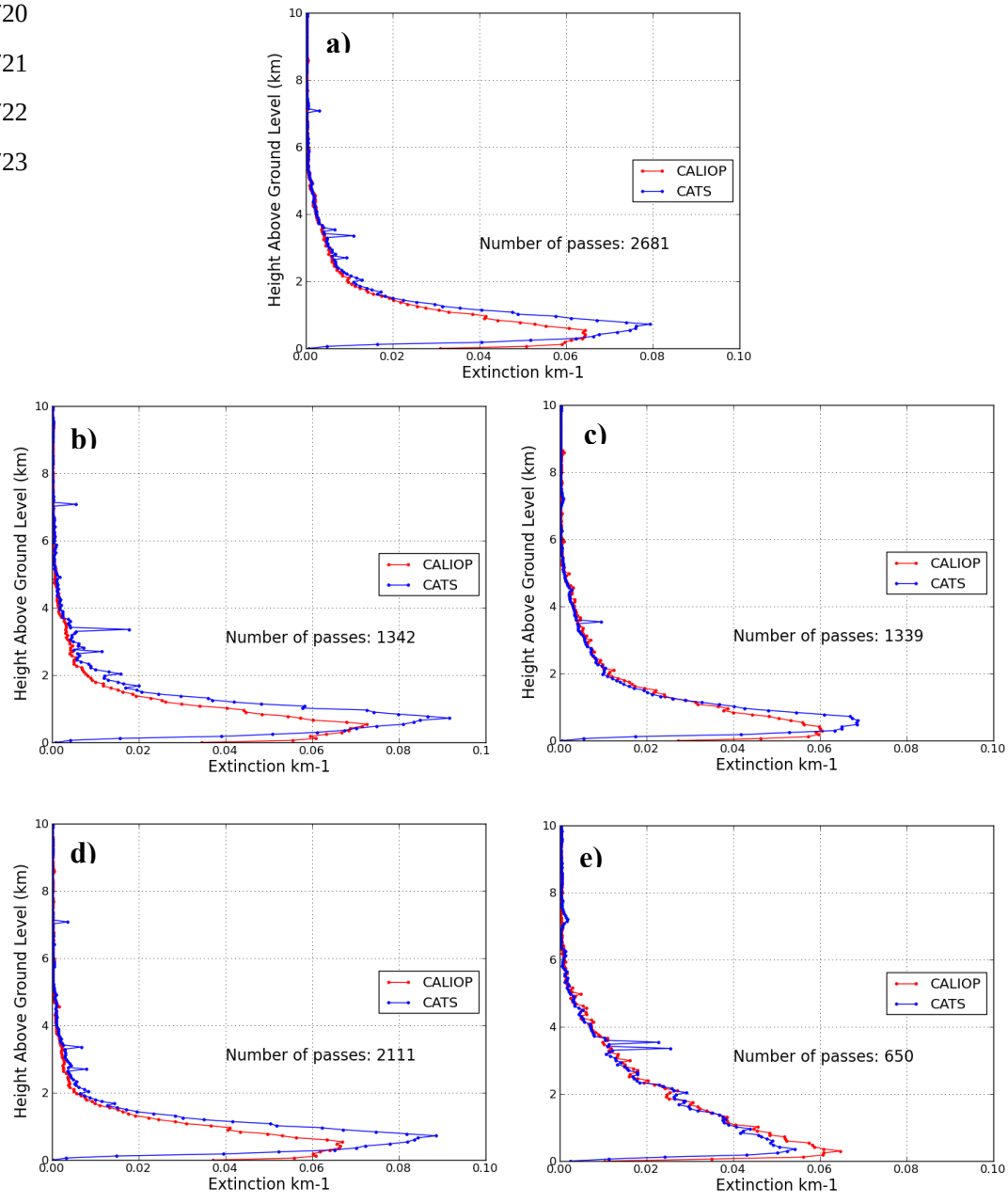

Figure 5. CATS and CALIOP vertical profiles of 1064 nm extinction for a) all profiles, b) daytime only, c) nighttime only, d) over-water, and e) over land.

Atmos. Chem. Phys. Discuss., https://doi.org/10.5194/acp-2018-1298
Manuscript under review for journal Atmos. Chem. Phys.
Discussion started: 20 December 2018

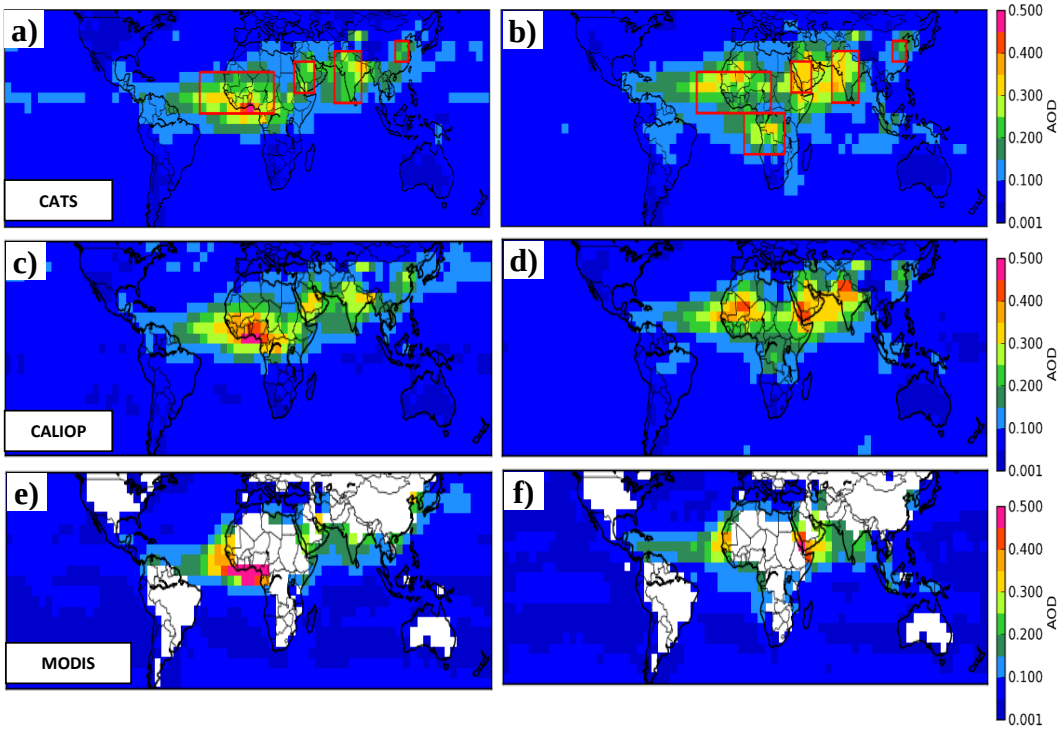

Figure 6. Mean AOD (1064 nm) by season for a) DJFMAM CATS, b) JJASON CATS, c) DJFMAM CALIOP, d) JJASON CALIOP, e) DJFMAM MODIS Aqua, and f) JJASON MODIS Aqua. Red boxes indicate locations of regional vertical distributions in Figures 12 and 13.

Atmos. Chem. Phys. Discuss., https://doi.org/10.5194/acp-2018-1298
Manuscript under review for journal Atmos. Chem. Phys.
Discussion started: 20 December 2018

731

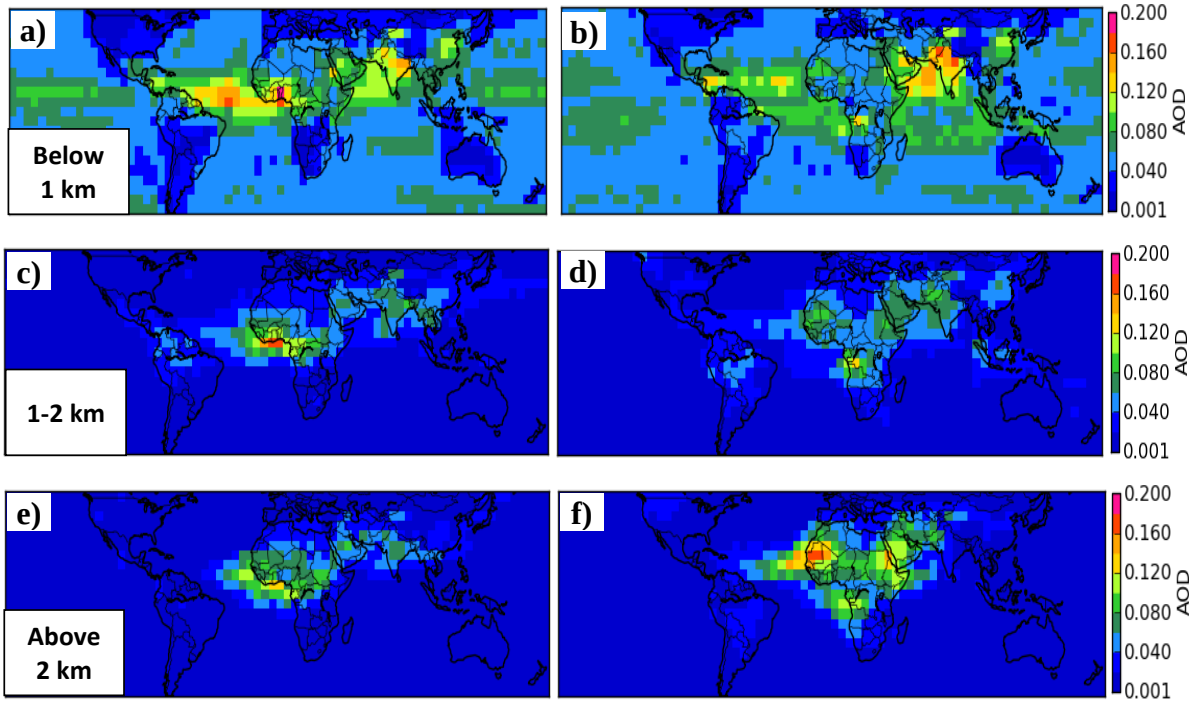

Figure 7: Mean CATS AOD (1064 nm) by season for a) DJFMAM below 1km AGL, b) JJASON below 1 km AGL, c) DJFMAM 1-2 km AGL, d) JJASON 1-2 km AGL, e) DJFMAM above 2 km AGL, and f) JJASON above 2 km AGL.

Atmos. Chem. Phys. Discuss., https://doi.org/10.5194/acp-2018-1298
Manuscript under review for journal Atmos. Chem. Phys.
Discussion started: 20 December 2018

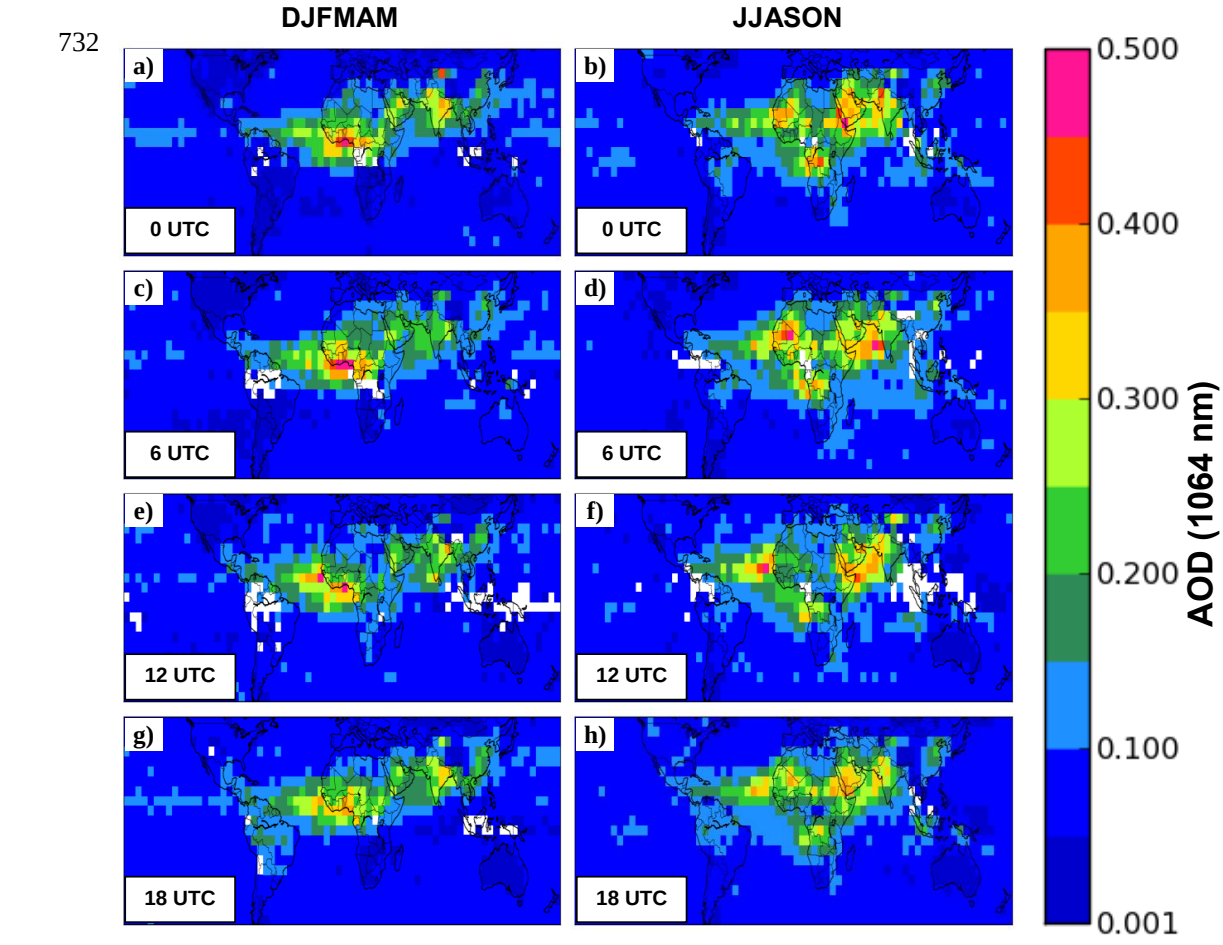

Figure 8. Seasonal Mean AOD (1064 nm) binned by every 6-hours for a) DJFMAM 0 UTC, b) JJASON 0 UTC, c) DJFMAM 6 UTC, d) JJASON 6 UTC, e) DJFMAM 12 UTC, f) JJASON 12 UTC, g) DJFMAM 18 UTC, and h) JJASON 18 UTC.

Atmos. Chem. Phys. Discuss., https://doi.org/10.5194/acp-2018-1298
Manuscript under review for journal Atmos. Chem. Phys.
Discussion started: 20 December 2018

733

734

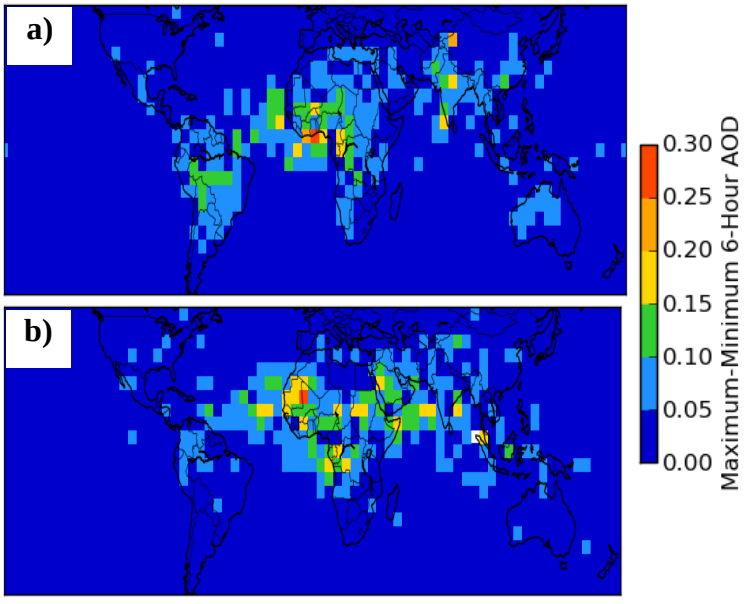

Figure 9. Maximum minus minimum mean seasonal AOD (1064 nm) for a) DJFMAM, and b) JJASON.

Atmos. Chem. Phys. Discuss., https://doi.org/10.5194/acp-2018-1298
Manuscript under review for journal Atmos. Chem. Phys.
Discussion started: 20 December 2018

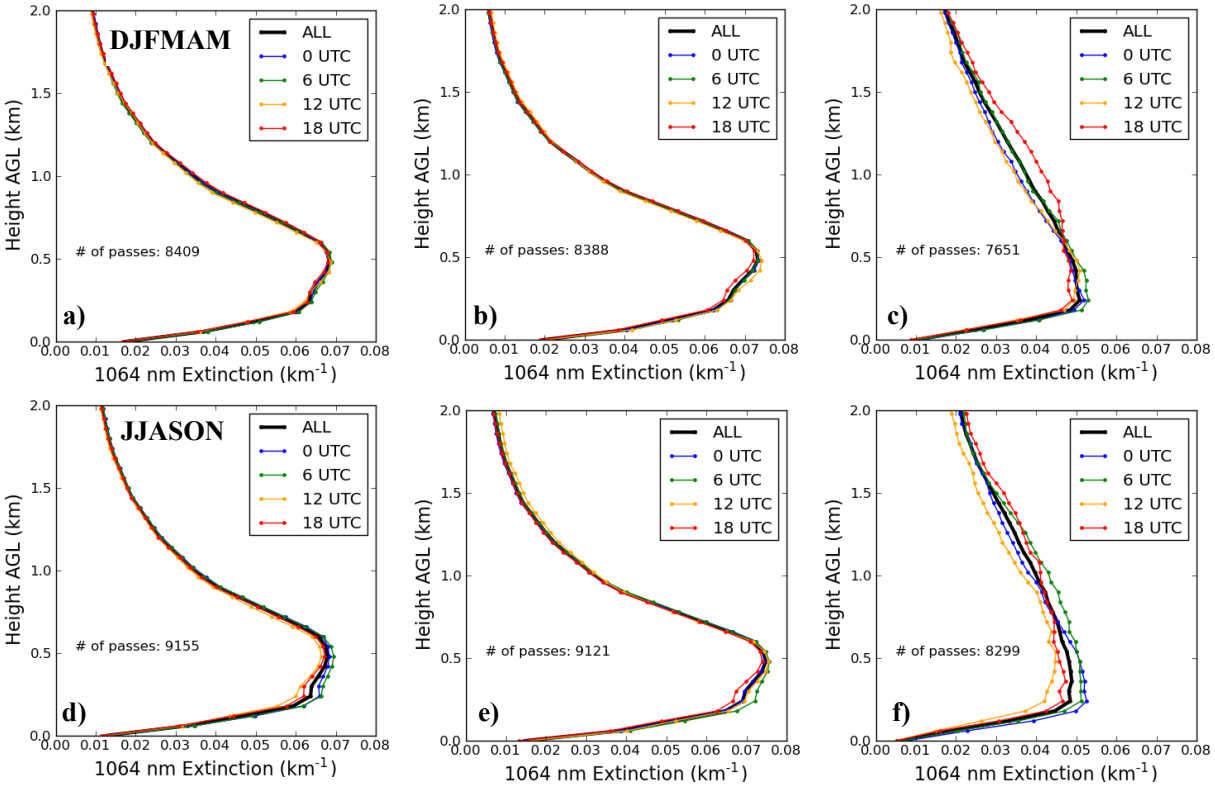

Figure 10. Global mean 6-hourly vertical profiles of CATS 1064 nm extinction for a) DJFMAM all profiles, b) DJFMAM water profiles, c) DJFMAM not-water profiles, d) JJASON all profiles, e) JJASON water profiles, f) JJASON not-water profiles.

Atmos. Chem. Phys. Discuss., https://doi.org/10.5194/acp-2018-1298
Manuscript under review for journal Atmos. Chem. Phys.
Discussion started: 20 December 2018

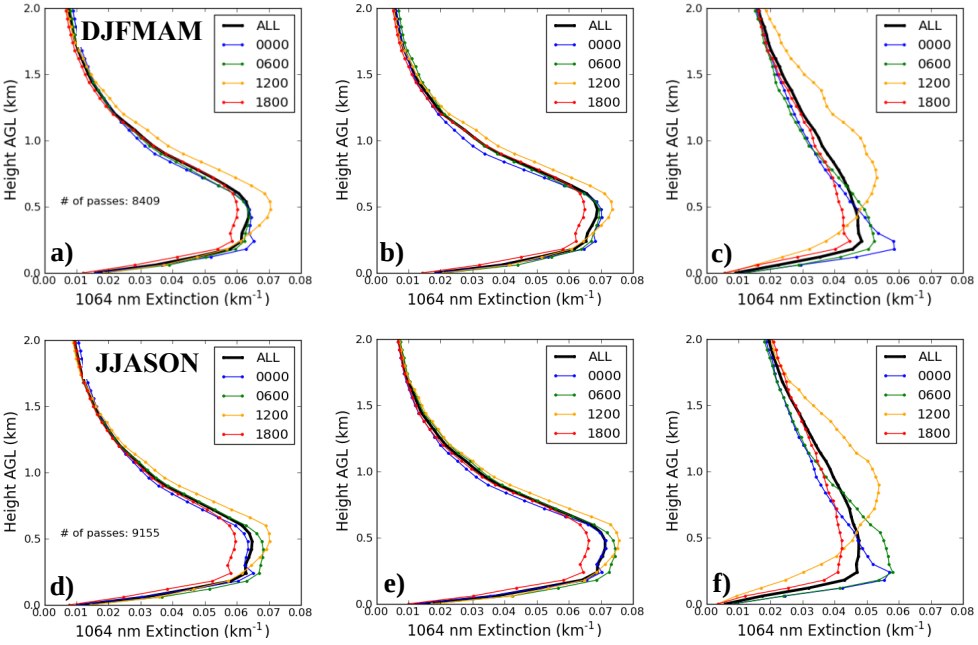

Figure 11. Global mean 6-hourly local time (0:00 am, 6:00 am, 12:00 pm and 6:00 pm) vertical profiles of CATS 1064 nm extinction for a) DJFMAM all profiles, b) DJFMAM water profiles, c) DJFMAM not-water profiles, d) JJASON all profiles, e) JJASON water profiles, f) JJASON not-water profiles.

Atmos. Chem. Phys. Discuss., https://doi.org/10.5194/acp-2018-1298
Manuscript under review for journal Atmos. Chem. Phys.
Discussion started: 20 December 2018

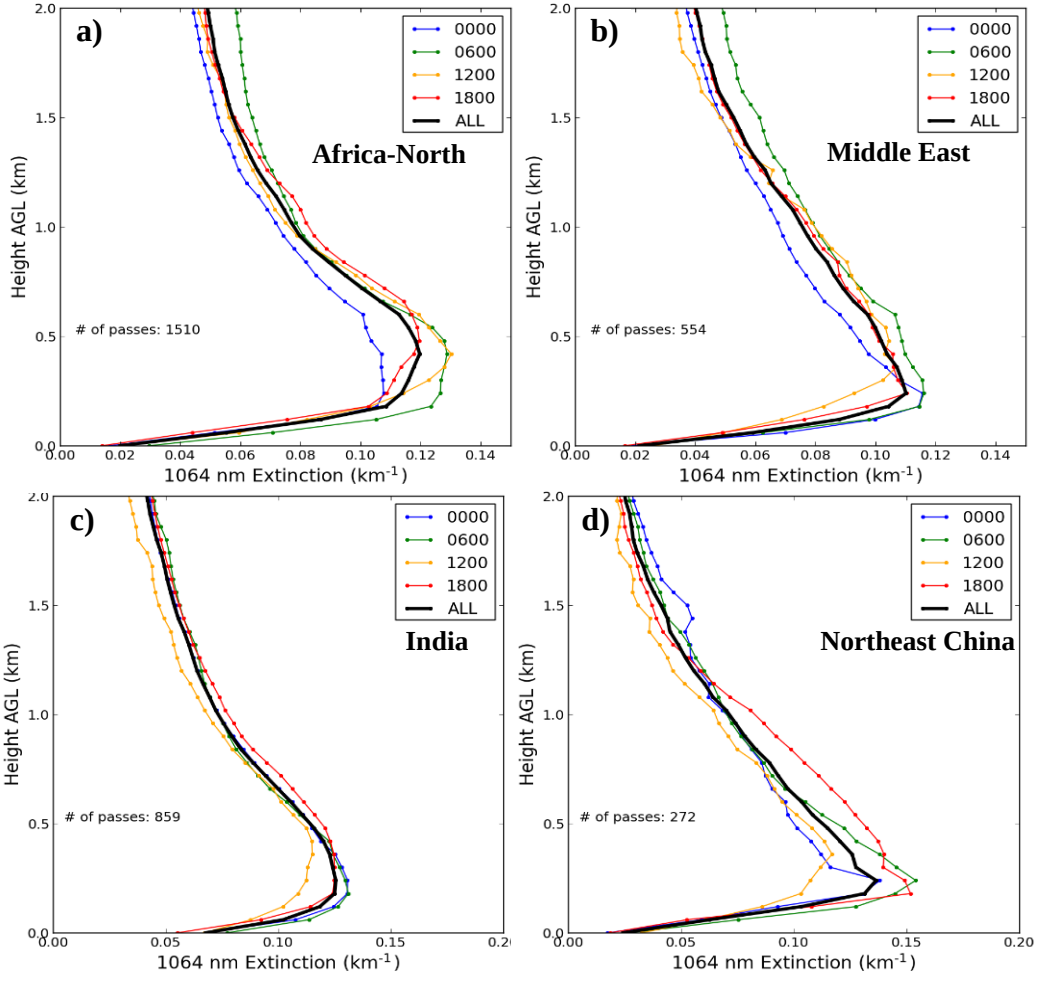

Figure 12. DJFMAM 6-hourly average (local time; 0:00 am, 6:00 am, 12:00 pm and 6:00 pm) vertical profiles of CATS 1064 nm for locations shown in Figure 6a; a) Africa-north, b) Middle East, c) India, and d) Northeast China.

Atmos. Chem. Phys. Discuss., https://doi.org/10.5194/acp-2018-1298
Manuscript under review for journal Atmos. Chem. Phys.
Discussion started: 20 December 2018

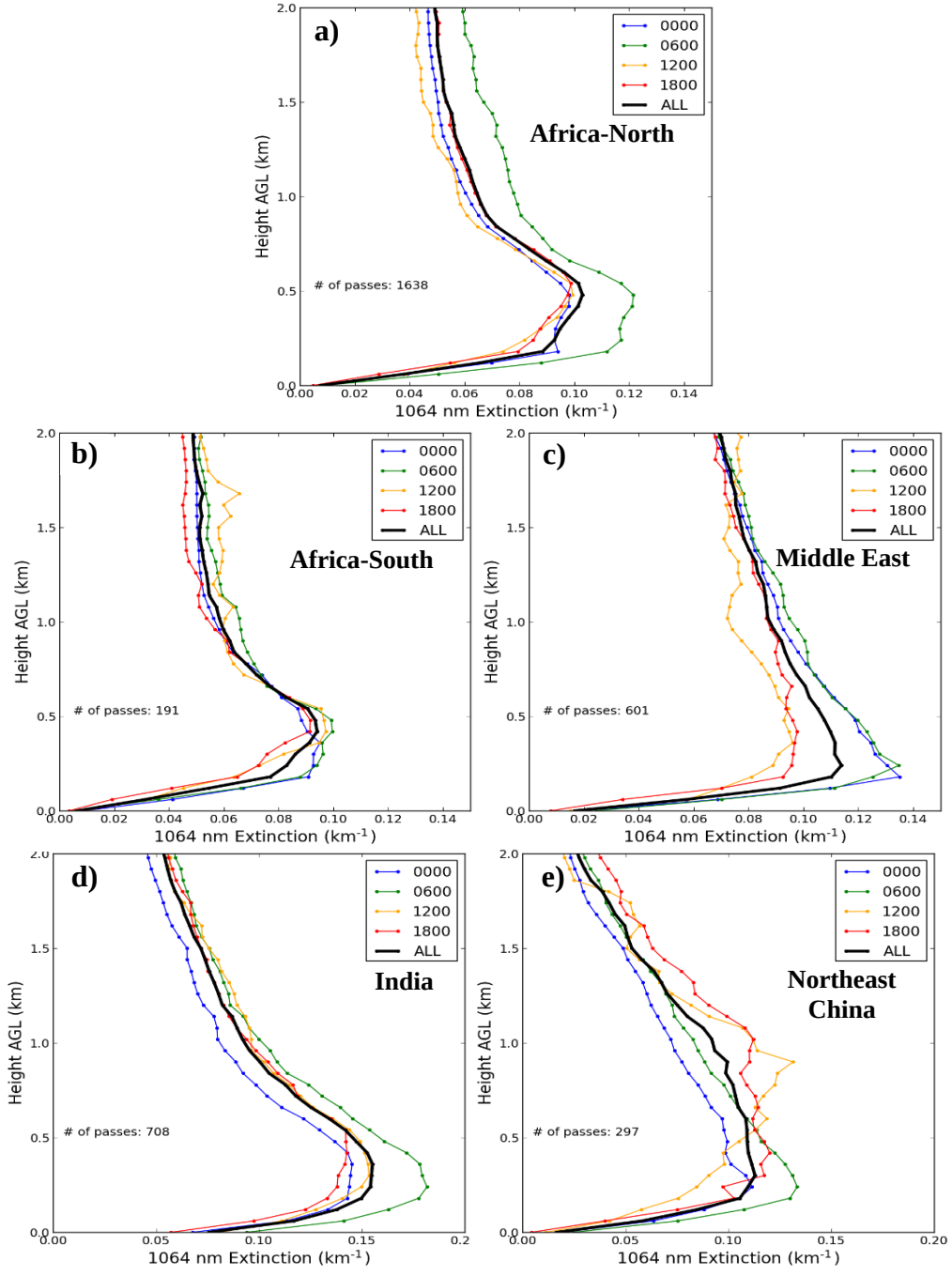

Figure 13. JJASON 6-hourly average (local time; 0:00 am, 6:00 am, 12:00 pm and 6:00 pm) vertical profiles of CATS 1064 nm for locations shown in Figure 6b; a) Africa-north, b) Africa-south, c) Middle East, d) India, and e) Northeast China.